

Dislocation microstructures in Si plastically deformed at RT

This article has been downloaded from IOPscience. Please scroll down to see the full text article.

2000 J. Phys.: Condens. Matter 12 10059

(<http://iopscience.iop.org/0953-8984/12/49/305>)

View [the table of contents for this issue](#), or go to the [journal homepage](#) for more

Download details:

IP Address: 171.66.16.221

The article was downloaded on 16/05/2010 at 07:04

Please note that [terms and conditions apply](#).

Dislocation microstructures in Si plastically deformed at RT

J Rabier[†], P Cordier[‡]§, T Tondellier[†], J L Demenet[†] and H Garem[†]

[†] Laboratoire de Métallurgie Physique, UMR 6630 CNRS, Université de Poitiers, SP2MI, BP 30179, 86962 Futuroscope Chasseneuil Cedex, France

[‡] Laboratoire de Structure et Propriétés de l'Etat Solide, ESA CNRS 8008,

Université des Sciences et Technologies de Lille, Bâtiment C6, 59655 Villeneuve d'Ascq Cedex, France

§ Bayerisches Geoinstitut, Universität Bayreuth, Germany

E-mail: jacques.rabier@lmp.univ-poitiers.fr

Received 13 September 2000

Abstract. Dislocation microstructures induced by plastic deformation at room temperature in Si have been investigated by TEM. Plastic deformation has been obtained by using two types of technique: deformation under a confining pressure of 5 GPa in an anisotropic multi-anvil apparatus and by surface scratching. The TEM observations show common features in the two deformation substructures which are characteristic of high stress–low temperature deformation. The deformation microstructures are built with dislocations with $a/2(110)$ Burgers vector in (111) planes which are undissociated. Such dislocations are mainly aligned along the screw orientation and $\langle 112 \rangle$ orientations at 30° from the Burgers vectors as well as along $\langle 132 \rangle$ orientations at 41° from the Burgers vector. The occurrence of those Peierls valleys confirms that different dislocation core configurations from those usually dealt with at higher temperatures have to be taken into account when dislocations are nucleated at very high stresses.

1. Introduction

In the context of a possible core configuration transition between dissociated glide and perfect shuffle dislocation in Si which can occur at high stress it is of interest to study specific deformation conditions yielding dislocation nucleation at low temperature. Indeed by calculating the activation energy required for double kink nucleation taking Peierls stresses into account, Duesbery and Joos [1] have shown that a dissociated dislocation in the glide set has a lower activation energy than a perfect dislocation in the shuffle set in the usually investigated range of stress. Extrapolation of their data at high stress shows that the transition between the two mechanisms should occur for stresses close to 0.01μ (μ shear modulus) i.e. about 500 MPa.

Low temperature macroscopic plastic deformation of silicon has been reported recently [2] at 150°C using an anisotropic multi-anvil apparatus under a confining pressure of 5 GPa, a confining pressure lower than that of the phase transition encountered during micro-indentation tests [3, 4]. In these deformation conditions the deformation microstructure has been found to be built with perfect dislocations and unexpected $\langle 112 \rangle/30^\circ$ Peierls valleys. Those features could be consistent with a deformation mechanism controlled by perfect shuffle dislocations which is expected at high stress extrapolating the calculations of Duesbery and Joos [1].

In this paper we report on the deformation microstructures obtained at RT using two different deformation techniques: deformation under a confining pressure of 5 GPa in an

anisotropic multi-anvil apparatus and by surface scratching. This last test has been widely used in the past (see, for example [5]) for introducing dislocations in Si. Usually a further annealing at high temperature under stress is used to move dislocations away from the scratch. However the characterization of dislocations nucleated at room temperature before any annealing, to our knowledge, has not been reported.

2. Experiment

2.1. High pressure deformation experiments

Si samples (FZ material, intrinsic $\rho = 800 \Omega \text{ cm}$) have been cut in the form of parallelepipeds $3.5 \times 2 \times 2 \text{ mm}^3$ with $[32\bar{1}]$ orientation axis. The surfaces have been mechanically polished (down to a final polish with $1 \mu\text{m}$ diamond powder). They were fitted into an aluminium jacket with an outer diameter of 3.2 mm which acts as a pressure medium transmitter.

In order to obtain plastic deformation at low temperature under known high confining pressure, a multi-anvil apparatus has been used in which the solid confining medium has been made anisotropic by adding two alumina rams at the ends of the sample [6]. By this technique it is possible to get a large deviatoric stress superimposed on a known large hydrostatic pressure.

The applied pressure around the sample was raised at a rate of 1 GPa h^{-1} up to 5 GPa. As a consequence of the design of the solid confining medium, a uniaxial stress is also built up during the pressure application. In these conditions the deformation rate can be roughly estimated to be $5 \times 10^{-5} \text{ s}^{-1}$. When the nominal pressure is reached, the pressure is maintained for one hour. Then the confining pressure is slowly released (during 15 h) in order to minimize the crack nucleation during this part of the test. Using this procedure, Si oriented along $[32\bar{1}]$ has been successfully plastically deformed at RT and plastic strains as large as 20% were obtained.

2.2. Scratch tests

The intrinsic Si sample used for scratching was cut from a (001), 0.650 mm thick, commercial wafer. After orientation, a scratch was made at RT on the (001) surface along a $\langle 110 \rangle$ direction, using a diamond scribe. The applied load was 0.45 N. This technique has been used in the past to study the dislocation mobility as a function of stress and temperature [5]. In the present case, no additional stress application or subsequent annealing were performed.

It is well known that a scratch along a $\langle 110 \rangle$ direction on a (001) surface leads mainly to dislocation generation on the two $\{111\}$ planes which have a common direction perpendicular to the scratch.

2.3. TEM characterizations

The sample deformed under high pressure was left within the aluminium jacket and slices were cut out of the sample using a diamond saw. In order to prevent those slices falling apart during the subsequent manipulations owing to the high crack density, they were impregnated with epoxy and then mechanically polished down to $120 \mu\text{m}$. Then the slices were dimpled down to $40 \mu\text{m}$ and ion milled at room temperature in a Gatan Duo Mill apparatus.

After scratching, the sample was thinned and polished by the back face, ground down to $120 \mu\text{m}$ then dimpled down to $40 \mu\text{m}$. The electron transparency was obtained by ion milling at RT on the back face for 4 h and finally on both faces for 1/4 h.

Thin foils were observed in a JEOL 200CX microscope operating at 200 kV.

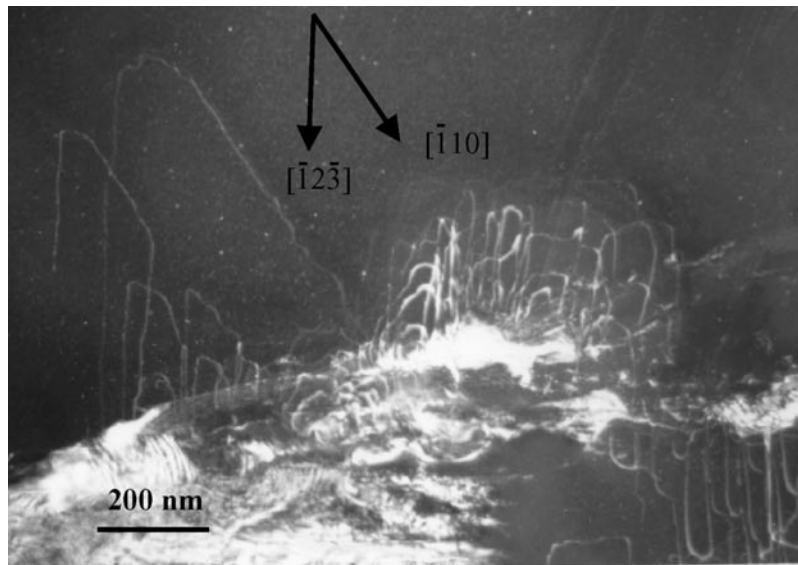


Figure 1. Microstructure of Si, plastically deformed along $[32\bar{1}]$ (RT, 5 GPa) shown in the (111) plane, weak beam dark field, $g = \bar{2}20$, $5g$ excited. Dislocations with $\frac{1}{2}[\bar{1}10]$ Burgers vector are undissociated and lie along the screw direction and the $[\bar{1}3\bar{2}]/41^\circ$ direction.

3. Results

3.1. Deformation microstructure after RT deformation under 5 GPa

The procedure described in section 2.1 results in a plastic deformation of the sample of about 20%. The deformation microstructure consists of numerous small cracks associated with dislocations. There is no evidence that cracks which form during the deformation are initiated by dislocation interaction occurring during plastic deformation. It is more likely that cracks are formed in the early stage of the deformation–pressurization process and that their extension is stopped when the pressure increases. Then they act as internal surfaces when stress increases which provide sources for dislocation nucleation [7]. This can be seen in figure 1 where dislocations are emitted from free surfaces of cracks. This figure is representative of the plastic deformation events found after RT deformation. Tilting experiments have been performed in order to determine the geometrical features of this microstructure. Glide loops lying in the (111) plane have a $\frac{1}{2}[\bar{1}10]$ Burgers vector and expand leaving behind screw segments as well as $\langle 123 \rangle$ segments. Those directions appear to be deep Peierls valleys for the dislocations. Narrow glide loops are built with only long $\langle 123 \rangle$ segments (see figure 1) and are connected by small dislocation segments having a non-directional character. These $\langle 123 \rangle$ directions located at 41° from the Burgers vector are close to the $\langle 112 \rangle/30^\circ$ direction reported before after deformation in the same conditions but at 150°C [2]. Only one slip system has been evidenced in this area although several slip systems have been found activated in other parts of the specimen. Twins, which usually result from large stress application, have not been evidenced. No dissociation as well as no local wide dissociation (nose) often reported after high stress deformation [8] have been resolved by using the weak beam technique.

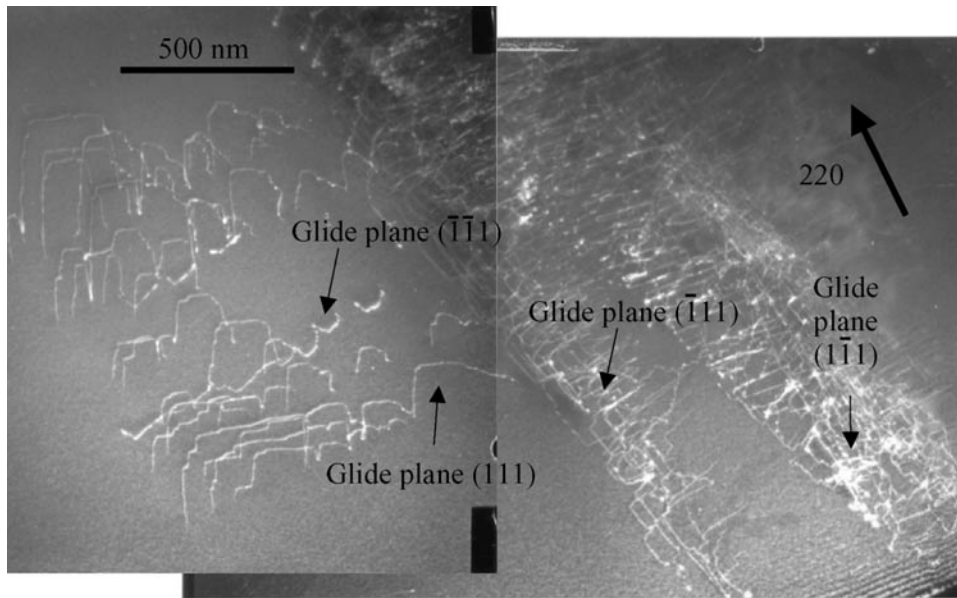


Figure 2. General view in the (001) plane of the microstructure after scratching along the [110] direction. The trace of the scratch is close to the top right corner of the micrograph. Weak beam dark field, $g = 220$, $3g$ excited. Dislocations lie on the four possible $\{111\}$ planes.

3.2. Deformation microstructure after scratching at RT

A general view of the microstructure resulting from the scratching procedure described in section 2.2 is shown in figure 2. Due to the experimental conditions, dislocations did not expand far from the scratch which is close to the top right corner of the micrograph, along the [110] direction. By conventional diffraction experiments, dislocations have been found to lie on the two expected glide planes, i.e. (111) and $(\bar{1}\bar{1}1)$, and also on the two other $\{111\}$ planes. Observations on the (001) plane (figure 2) show that these dislocations form half loops with straight segments on each glide plane. In order to determine the orientation of those segments, the thin foil has been tilted towards the $\{111\}$ planes. In figure 3, only one slip system is evidenced. Dislocations have a $\frac{1}{2}[0\bar{1}1]$ Burgers vector and lie on the (111) plane. Half loops are composed of segments mainly aligned along crystallographic directions. Some narrow half loops are aligned along the $[\bar{2}\bar{1}3]$ direction, and the others are composed of $\langle 123 \rangle$ and screw segments. The high density of dislocations prevents precise determination of the orientation of the connecting segments. However some of them are seen aligned along $\langle 123 \rangle$ and/or $\langle 112 \rangle$ directions. Same crystallographic directions (screw, $\langle 123 \rangle$ and $\langle 112 \rangle$) have been evidenced in other glide planes which bears witness that these directions are Peierls valleys for dislocations at room temperature.

No dissociation has been found using the weak beam technique.

4. Discussion

Usual higher temperature deformation microstructures ($420^\circ\text{C} < T < 700^\circ\text{C}$) [8] exhibit dislocations with $\frac{1}{2}\langle 110 \rangle$ Burgers vectors dissociated into two Shockley partials and located along $\langle 110 \rangle$ directions in a $\{111\}$ glide plane building hexagonal glide loops. In the present

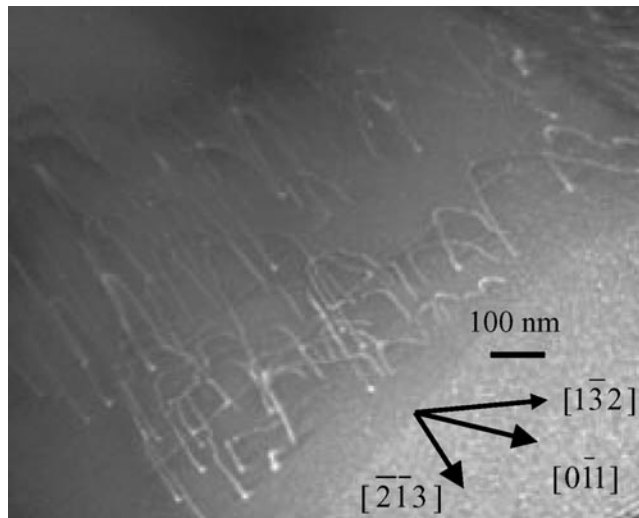


Figure 3. Half loops of dislocations with a $\frac{1}{2}[0\bar{1}1]$ Burgers vector lying on the (111) plane. Segments are mainly aligned along the screw and $[\bar{2}13]$ directions. Weak beam dark field, $g = 022$, $3g$ excited.

study the microstructure is built with perfect dislocations with $\frac{1}{2}\langle 110 \rangle$ Burgers vectors which are locked within Peierls valleys corresponding mainly to screw orientation, $\langle 112 \rangle/30^\circ$ orientation and $\langle 123 \rangle/41^\circ$ orientation. $\langle 112 \rangle$ valleys have been already reported in indented Si in very deformed regions [9]. Such segments have been also observed after deformation under confining pressure [10] at 425°C , but have been proved to be in fact segments lying along $\langle 110 \rangle$ directions in the cross slip plane. Tilting experiments show that those segments evidenced here are clearly located in the glide plane. Such $\langle 112 \rangle/30^\circ$ orientations are unexpected for dissociated dislocations in the glide set but are consistent with low energy directions for perfect dislocations in the shuffle set. This was derived a long time ago by Hornstra [11] on the basis of geometrical considerations, i.e. number of broken bonds per unit length of dislocations. Indeed in terms of perfect shuffle dislocation the $\langle 112 \rangle/30^\circ$ dislocation appears to have the lowest density of broken bonds. However the reconstruction of those bonds is as complex as their density is low. The further apart the dangling bonds are, the more difficult the reconstruction. Taking into account possible reconstruction shows that $\langle 123 \rangle/41^\circ$ orientations are more likely to be the actual Peierls valleys rather than $\langle 112 \rangle/30^\circ$ orientations. Indeed it corresponds to an average direction of a kinked $\langle 112 \rangle/30^\circ$ where reconstruction could be easier at the kink positions. This will be discussed in a forthcoming paper [7].

5. Conclusion

RT plastic deformation of silicon has been obtained macroscopically by deformation under a confining pressure of 5 GPa, as well as locally around surface scratches. In these two deformation conditions original deformation microstructure appears as compared to what is seen at temperatures larger than 400°C . The substructure does not seem to depend on the actual deformation conditions since the observations are comparable in the two sets of experiments. Dislocations are seen undissociated without any evidence of large local splitting events as reported usually under high stress experiments [8]. This is consistent with a deformation

mechanism by perfect shuffle dislocations expected from calculations [1] at high stress. They are associated with $\langle 112 \rangle / 30^\circ$ and $\langle 123 \rangle / 41^\circ$ Peierls valleys which appear to be characteristic of high stress and low temperature. These observations could be consistent with the occurrence of a plastic deformation controlled by perfect shuffle dislocations. The occurrence of $\langle 112 \rangle / 30^\circ$ and $\langle 123 \rangle / 41^\circ$ Peierls valleys appears consistent with this hypothesis as these directions can be low energy locations for unreconstructed and reconstructed perfect shuffle dislocations.

Acknowledgments

High pressure experiments were performed at the Bayerisches Geoinstitut under the EU 'TMR—large scale facilities' programme (contract No ERBFMGECT980111 to D C Rubie).

References

- [1] Duesbery M S and Joos B 1996 *Phil. Mag.* A **74** 253
- [2] Rabier J, Cordier P, Demenet J L and Garem H 2000 *Proc. Int. Congr. 'Dislocations 2000' (Gaithersburg, MD 2000) Mater. Sci. Eng. A* at press
- [3] Gridneva I V, Milman Yu V and Trefilov V I 1972 *Phys. Status Solidi* a **14** 177
- [4] Suzuki T and Ohimura T 1996 *Phil. Mag.* A **74** 1073
- [5] George A and Champier G 1979 *Phys. Status Solidi* a **53** 529
- [6] Cordier P and Rubie D 2000 *Proc. Int. Congr. 'Dislocations 2000' (Gaithersburg, MD 2000) Mater. Sci. Eng. A* at press
- [7] Rabier J *et al* to be published
- [8] Wessel K and Alexander H 1979 *Phil. Mag.* **35** 1523
- [9] Hill M J and Rowcliff D J 1974 *J. Mater. Sci.* **9** 1569
- [10] Veyssiere P, Rabier J, Demenet J L and Castaing J 1984 *Deformation of Ceramic Materials II* ed R Tressler and R C Bradt (New York: Plenum) p 37
- [11] Hornstra J 1958 *J. Phys. Chem. Solids* **5** 129